Effect of high rebar temperature during casting on corrosion in carbonated concrete

Lijie Chen and Ray Kai Leung Su*

Department of Civil Engineering, The University of Hong Kong, Pokfulam Road, Hong Kong, China

Abstract: The heated bar effect on the corrosion rate, corrosion potential and resistivity of partially carbonated concrete is discussed in this paper. The potential use of pulverized fuel ash (PFA) as a substitute for cement to mitigate the heated bar effect is explored. It is found that the heated bar effect can lead to an increase in the corrosion level. The moisture content within concrete noticeably affects the heated bar effect on the corrosion performance of partially carbonated concrete.

Keywords: heated bar effect; corrosion rate; reinforced concrete; pulverized fuel ash; carbonation; steel-concrete interface

1. Introduction

Corrosion caused by the dissolution of the passive film on the reinforcement surface is an important issue to address in concrete durability problems. The stability of the passive film in a highly alkaline concrete pore solution can be affected by the carbonation of the concrete or chloride ion attacks. Previous studies [1-3] have found that the properties at the steel-concrete interface (SCI) have direct effects on the corrosion performance of reinforced concrete (RC) which lead to depassivation of the reinforcements. Jeanty et al. [4] were the first to investigate

* *Corresponding author, Email: klsu@hku.hk, Tel no.: +852 2859 2648*

defects at the SCI caused by the top bar effect. They found the RC beams cast from top to bottom have less structural strength and stiffness than those cast from bottom to top. The degradation of the structural performance is believed to be induced by the SCI defects on top bars during the top-bottom casting. Zhang et al. [5] used a video-microscope and observed voids under the top rebar. The segregation, settlement and bleeding of fresh concrete become more significant with increases in the height of the rebar, which leads to remarkable increases in voids. As a result, the corrosion pattern of the top rebar changes; that is, instead of pitting corrosion, generalized corrosion occurs due to the chloride attack. The interfacial defects induced by the top bar effect also increase the overall corrosion rate in carbonated concrete [6, 7]. However, the top bar effect can be mitigated by casting concrete vertically [2] or using self-compacting concrete [8].

The durability of RC structures can also be influenced by the effects of heated rebars. Pati [9] found that an increase in the rebar temperature significantly reduces the pull-out strength of RC, and pulverized fuel ash (PFA) used to partially replace cement mitigates the effect of temperature on the pull-out strength of the rebars. The pore diameter and total porosity of the concrete near the SCI increase due to the thermal effects on the rebars.

The heat from solar radiation could increase the rebar temperature up to 80^{o}C in the summer of the USA [9]. The temperature of rebars would be further increased concerning longer summers and higher temperatures due to global warming, especially in the tropical and subtropical regions and countries, such as Southeast Asia, Africa and the USA. There is considerable knowledge on casting concrete in hot weather and there are common related practices worldwide. However, knowledge related to the effects of high rebar temperature during the casting of concrete (heated bar effect) on the microstructure of the SCI is limited. The defects at the SCI caused by the heated bar effect and subsequent deterioration of the corrosion performance have not been investigated.

The impacts of defects at the SCI due to the heated bar effect with respect to the corrosion behaviors of carbonated concrete are investigated in this study. Here, the effect caused by an increase in the temperature of the rebar during concrete casting is referred to as the heated bar effect. Accelerated carbonation is used to depassivate the reinforcements in the concrete. The effects of the water-cement (w/c) ratio and concrete constituents on the corrosion rate, corrosion potential and concrete resistivity are experimentally studied. The potential of using PFA to mitigate the heated bar effect is also explored.

2. Experimental procedures

2.1. Specimen design

A total of 6 specimens were tested in an experimental program to examine the effect of increases in the rebar temperature on the durability of concrete. The properties of the specimens are listed in Table 1. The depassivated rebars were subjected to carbonation afterwards while the passive film of the passivated rebars would remain stable all the time. The depassivated rebars were heated to a desired temperature in an oven to ensure even heat distribution prior to concrete casting. On the contrary, the passivated rebars were maintained at an ambient temperature. The first specimen in each group was used as the reference while the second specimen was used in the experiment. The heated bar effect was examined by comparing the reference specimen with the experimental specimen. In order to minimize possible variations caused by random factors, the concrete casting process, exposure environment, and measurement scheme were the same for each group of specimens.

The chemical composition of the binders and mix proportions for a cubic meter of concrete are shown in Table 2 and 3 respectively. The specimen dimensions are 100×100×300 mm with a concrete cover of 10 mm. The steel reinforcements are Grade 500B rebars with a

diameter of 10 mm. The existing rust on the rebars was removed with an iron wire brush prior to heating. All of the specimens were cast longitudinally rather than in the conventional transverse direction to minimize the top bar effect, as shown in Figure 1(a). A plastic plate with two holes was installed to fix the rebars into position during the vibration test. The specimens were cured in air for 28 days and the formwork was removed in the first 24 hours after concrete casting.

An identical specimen was casted for each specimen, and stored in the same accelerated carbonation chamber to determine the depth of the carbonation.

2.2. Accelerated carbonation test

After curing, the side and top surfaces of the specimens were covered with tape and epoxy resin to ensure that carbon dioxide (CO_2) could only penetrate through the surface at the bottom of the specimen, as shown in Figure 1(b). The specimens were placed in an accelerated carbonation chamber. The CO_2 concentration, temperature and relative humidity in this chamber were controlled at 50%, 20℃ and 65%, respectively.

The additional specimens were used instead of the test specimens to measure the depth of the carbonation. A hole was bored on the bottom surface of the additional specimens, and the extracted powders were collected into the test tube with the help of the funnel as shown in Figure 2(a) and 2(b). During the drilling process, the powders were sorted according to the depth from the concrete surface. Thus, the sorted powders in the test tube can reflect the carbonation depth within the drilled hole. The depths of drilled hole and powders in the test tube were measured after drilling. A phenolphthalein test was conducted to measure the carbonation depth with the sorted powder from the drilled hole. The ratio of the depth of the drilled hole to that of the sorted powders is used to scale the carbonation depth with the sorted powders. Therefore, the carbonation depth with the drilled hole is obtained. The hole was filled

with plaster immediately after drilling to prevent the potential variations of the carbonation depth around the hole. Every 7 days, a hole was drilled on the surface of the bottom of the specimen, as shown in Figure 2(c). Once the carbonation front fully exceeded the depassivated rebar, the accelerated carbonation testing of both the test and additional specimens was stopped and the specimens were ready to undergo corrosion measurement.

Figure 3 shows the carbonation depth of each group of specimens for different exposure times. For the Group 1 specimens, the accelerated carbonation test was carried out for 9 weeks, at an average carbonation rate of 2.2 mm/week. The carbonation rate of the Group 2 specimens is much higher than that of Group 1 due to the higher w/c ratio. The average carbonation depth of the Group 2 specimens is 28.4 mm within the first week of the accelerated carbonation test, so this group of specimens was removed from the carbonation chamber after the first week. The carbonation rates of the Group 3 specimens are quite different among themselves due to the partial replacement of cement with PFA. Specimen 3-1 with a w/c ratio of 0.6 was carbonated at a rate of 2.6 mm/week which is similar to the results of the Group 1 specimens. However, only 1 week was necessary for Specimen 3-2 to reach a carbonation depth of 28.6 mm. At the end of the accelerated carbonation testing of Specimen 1-1, unidirectional carbonation was confirmed on the specimen. The tape and resin on the top surface of Specimen 1-1 (the additional specimen) were removed, and the phenolphthalein test results of the powder collected from the concrete close to the surface showed that no CO_2 has penetrated through the top surface.

2.3. Corrosion behavior evaluation

For the corrosion measurements, the tape and epoxy resin on the test specimens were removed except for those on the end parts of the rebars. The specimens were then subjected to

drying-wetting cycles. Each drying cycle lasted for 6 days followed by a wetting cycle of 1 day. During the wetting cycle, the specimens were placed in an airtight container and immersed into tap water. During the drying cycle, the specimens were exposed to an average ambient temperature of about 22.7℃ (20℃ - 25℃) and average relative humidity of 66.8% (49%-83%). Three points for measurement were marked longitudinally near the depassivated and passivated rebars, as shown in Figure 4. Each point was measured three times for each measurement during the drying cycle. The corrosion rate, corrosion potential and concrete resistivity of the specimens were measured with a testing device for evaluating corrosion [10]. Temperature compensation was considered. The corrosion rates were obtained by interpreting the measured linear polarization resistance of the rebars by using the Stern-Geary equation [11, 12]. The total exposure period of the drying-wetting cycles was 81 and 150 days for Groups 1 and 2 respectively. Although the two specimens in Group 3 were cast simultaneously, the drying-wetting cycles of Specimen 3-1 started later than Specimen 3-2 because of the difference in the accelerated carbonation period. The total exposure time of Specimens 3-1 and 3-2 was 95 and 143 days respectively. Measurements of Specimen 3-2 were selected on the 0 to the 95^{th} day for comparison purposes with Specimen 3-1 which is discussed in the following sections.

3. Experimental results

3.1. Corrosion rate

Figure 5 shows the sum of the average corrosion rate of the rebars in all three groups. Half of the rebars are moderately corroded while the corrosion rate of the other half ranges from 1.0 to 3.22 uA/cm^2, thus indicating a high level of corrosion based on Table 4. However, it should be noted that there might be overestimations of the corrosion rate of passive reinforcements which have a small diameter under saturated conditions by the corrosion testing device used in this study [10]. If the concrete resistivity is low enough (e.g. less than 200 ohm×m) and the

polarization resistance of the reinforcement is high, more of the current generated by the outer probes would flow through the concrete between the outer probes rather than the reinforcement with a low frequency current. The different current flow paths between high and low frequency currents contradict the assumption of the corrosion testing device used in this study [10]. In this study, the reinforcements are 10 mm in diameter. Furthermore, all specimens are measured under cyclic drying-wetting cycles. This explains why the measured corrosion rates of the passivated rebars are higher than expected. Despite the overestimation of the passivated rebars in this study, it is still possible to use the corrosion rate of the passivated rebars as reference. As for the actively corroding reinforcements, the measured corrosion rate is considered to be accurate enough even in saturated conditions [10].

The heated bar effect is evidenced by the higher corrosion activity in Groups 1 and 2. The increase in the corrosion rate in Groups 1 and 2 due to the heated rebar effect is 27.3% and 32.5% respectively. On the other hand, the corrosion rate of Rebar 1-2-C-0.6-25-P decreases by 11.8% compared with that of Rebar 1-1-C-0.6-25-P. Rebar 2-1-C-1.0-25-P and 2-2-C-1.0-25-P corroded in a similar activity.

In Group 3, PFA was used to partially substitute the cement in Specimen 3-2, which has been concluded in previous studies as an effective supplementary material to increase the chloride resistance of concrete [13, 14]. However, the carbonation rate of Specimen 3-2 is significantly accelerated because of the lower pH buffering capacity (see Figure 3). The corrosion rate of the depassivated rebar in this PFA based specimen is almost twice that of the other samples. Therefore, PFA, used as a supplementary cementitious material to address carbonation which threatens the durability of concrete will increase the corrosion of the depassivated rebars and should be used with care.

3.2. Corrosion potential

Figure 6 presents the average corrosion potential of the rebars in all of the groups of specimens. Although corrosion potential is not quantitatively correlated to corrosion rate, higher corrosion activity can be identified by greater negative corrosion potential under similar conditions [15]. The corrosion potential of all of the depassivated rebars has less than a 90% corrosion probability in accordance with the ASTM C876 standard [16]. On the other hand, all of the passivated rebars show a higher corrosion potential at around -200 mV vs. Copper Sulfate Electrode (CSE), which corresponds to a 10% probability of corrosion. This proves the applicability of the test that uses unidirectional carbonation.

The overall trend of the corrosion activity in Groups 1 and 2 as indicated by the corrosion potential is the same as that of the corrosion rate. In comparison to the reference specimen, the corrosion potential of the depassivated rebars becomes more negative. On the contrary, the corrosion potential of the passivated rebars becomes more positive. The increase in the corrosion potential of the passivated rebars in Groups 1 and 2 may rule out the possibility that the increased corrosion levels of the depassivated rebars are caused by variations between two specimens within the same group. The corrosion potential of Rebar 1-2-C-0.6-70-D is reduced by 7.8% compared to that of Rebar 1-1-C-0.6-25-D. The corrosion potential of Rebars 2-1-C-1.0-25-D and 2-2-C-1.0-50-D is similar.

The corrosion potential of both the passivated and depassivated rebars in Specimen 3-2 is lower than those in Specimen 3-1. There is a notable reduction in the corrosion potential of the depassivated rebar in Specimen 3-2 compared to that in Specimen 3-1.

3.3. Concrete resistivity

The measured values of the average resistivity of the top and bottom surfaces of the concrete specimens are shown in Figure 7. Apart from the corrosion potential, the concrete resistivity provides supplementary information on the corrosion activity of RC structures [17].

Within concrete structures and in general, a lower resistivity value results in a higher risk of corrosion.

There are many factors that affect concrete resistivity such as cement type, w/c ratio, exposure conditions and carbonation [18, 19]. For OPC samples that have identical mix proportions, the resistivity value mainly depends on the microstructure and saturation state of the concrete. When concrete is exposed to CO_2, the precipitation of the calcium carbonate not only reduces the concentration of hydroxyl ions but also decreases the pore size in concrete [20], thus increasing the concrete resistivity. For the concrete specimens in which PFA is used to partially substitute for cement, their resistivity would increase due to the higher tortuosity from the hydration products of the PFA [21].

There are no significant differences between the resistivity values measured on the top and bottom surfaces near the passivated and depassivated rebars of the specimens in Group 1. This suggests that Specimens 1-1 and 1-2 have a similar pore structure and carbonation depth.

The resistivity near the depassivated rebar is increased by 14.2% compared to the reference specimen in Group 2. This trend contradicts the previous results based on the empirical relationship between corrosion rate and concrete resistivity. However, it should be noted that concrete resistivity may reflect the concrete saturation state [17] and the heated bar effect is supposed to be limited near the SCI because the heat would be consumed locally rather than dissipating to the bulk cement paste. In considering that the casting, curing and measurement procedures of these two specimens are the same and the increase in resistivity is minimal, a more reasonable interpretation of this increase in concrete resistivity is that the porosity and average pore saturation are both lower in the experimental specimen. Combined with the previous results, it can be concluded that the heated bar effect increases the corrosion rate of the depassivated rebar in the experimental specimen while lower corrosion activity as indicated by the corrosion potential of the passivated rebar in the experimental specimen is due

to lower pore saturation.

The increases in the concrete resistivity from carbonation and the partial replacement of cement with PFA are obvious in Group 3 when the measured resistivity value near Rebars 3-1-C-0.6-70-D and 3-2-P-0.6-25-P are compared with that near Rebar 3-1-C-0.6-25-P. The effect of carbonation on resistivity is significantly greater than when PFA is used as a supplementary material in this study. This is likely due to the increase in porosity resultant of the use of a large volume of PFA [22]. The measured concrete resistivity near Rebar 3-2-P-0.6-70-D is similar to that near Rebar 3-2-P-0.6-25-P. Thus, carbonation appears to have little influence on the resistivity of the PFA based specimen.

3.4. Correlations

Figure 8 shows the correlations among the corrosion rate, corrosion potential and concrete resistivity of all of the reinforcements. There is a relation of proportionality between the logarithms of the corrosion rate and concrete resistivity, in which lower concrete resistivity indicates a higher corrosion rate. This relationship has been identified in the results of many previous studies [17, 23, 24]. On the other hand, the corrosion potential is logarithmically proportional to the concrete resistivity. The R-squared values reveal that the corrosion rate-concrete resistivity relationship is a better fit compared to the corrosion potential-concrete resistivity relationship.

Figure 8(a) and 8(c) show that the corrosion rate-concrete resistivity relationships for the passivated rebars in Groups 1 and 2 are quite similar while for the depassivated rebars, the heated bar effect causes higher corrosion rates with lower concrete resistivity. As for Group 3, with the same resistivity, the corrosion rate of Rebar 3-2-P-0.6-70-D is lower than Rebar 3-1-C-0.6-70-D below 1000 Ohm·m as indicated by Figure 8(e). However, Rebar 3-2-P-0.6-70-D generally has higher corrosion activity than Rebar 3-1-C-0.6-70-D due to lower concrete

resistivity as mentioned before.

For the corrosion potential-concrete resistivity relationships in Group 1, the corrosion potential of the depassivated rebars is reduced by the heated bar effect when the concrete is under saturated or semi-saturated conditions. The corrosion potential of Rebar 2-2-C-1.0-50-D is generally lower than that of Rebar 2-1-C-1.0-25-D due to the increase in rebar temperature in Group 2. As for Group 3, the corrosion potential of Specimen 3-2 is substantially lower than that of Specimen 3-1 within the low range of resistivity values.

4. Discussion

The experimental results show that the heated bar effect results in the deterioration of the corrosion performance of RC. The corrosion rate of depassivated rebars in carbonated concrete can be controlled by three processes, namely anodic reaction, cathodic reaction of the reinforcements, and ion transport through the concrete [23]. Although Smith et al. [19] claimed that higher concrete resistivity increases the difficulty of ions in migrating through concrete and thus inhibits corrosion, Glass et al. [24] concluded that carbonation-induced corrosion is consistent with anodic resistive control; that is, anodic reactions are based on resistive control. The mechanism of carbonation-induced corrosion can be explained by using an Evans diagram [25]. Figure 5 and Figure 6 show that compared to the reference specimens, the corrosion rates increase with reduced corrosion potential for the depassivated rebars in Groups 1 and 3. This suggests that the change in the corrosion rate of the depassivated rebars is mainly due to higher anodic activity, viz. it is due to anodic control. In Group 2, the corrosion potential remains almost constant while the corrosion rate increases for the depassivated rebars, which might indicate higher activity of the anodic and cathodic reactions due to the heated bar effect.

The heated rebar effect on the corrosion performance of partially carbonated concrete is found to be dependent on the moisture content of concrete. Figure 9 shows the average increase

in corrosion rate of the depassivated rebars in Groups 1 to 3. The increase in the average corrosion rate shows a descending trend as the pore solution of the concrete changes from a saturated/semi-saturated to a relatively dry state. For Group 3, the higher porosity of the PFA based concrete leads to higher corrosion levels in the depassivated rebar. For Groups 1 and 2, the increase in the corrosion rate, on one hand, may be led by the increasing porosity near the SCI due to the heated rebar effect. This is supported by the mercury intrusion porosimetry (MIP) tests conducted by Pati [9], who shows that the pore diameter and total porosity near the SCI increase with higher rebar temperatures. The effects of relative humidity and porosity on the corrosion rate of rebars in carbonated concrete are significant and have been observed in many studies [24, 26, 27]. It has been concluded that the moisture content and the microstructure of the concrete determine the availability of electrolytes near the SCI and thus the corrosion rate in the corrosion propagation stage [26, 27]. On the other hand, the presence of Calcium Hydroxide (CH) near the SCI may be altered due to higher rebar temperature, which plays a critical role in resisting the carbonation-induced corrosion as a pH buffer. During the concrete casting process, the cement hydration near the SCI may be accelerated due to the heat dissipated by the heated rebar or inhibited by the water evaporation according to the Fourier transform infrared (FTIR) results of Pati [9]. Therefore, CH as the cement hydration product would be affected.

As a by-product of the coal industry, PFA when used in high volume as a supplementary material has great potential for achieving lower carbon emissions in the construction industry [28, 29]. The bond-strength degradation is resolved by partially substituting cement with PFA [9]. However, apart from the findings in some of the previous studies [22, 23, 30, 31], the use of PFA as substitute for cement has negative impacts on both the carbonation resistance and corrosion performance of the RC specimens in this study. The means of mitigating the heated bar effect on carbonation-induced corrosion in concrete structures need to be further

investigated.

5. Conclusions

The following conclusions are made based on the findings in this study:

1. The heated bar effect can be detrimental to the corrosion performance of carbonated concrete. High rebar temperatures lead to higher corrosion rates and lower corrosion potential of carbonated concrete.

2. The moisture content greatly affects the heated bar effect. Higher heated bar effect within the saturated concrete may be induced by higher electrolyte availability due to the SCI defects. However, the cement hydration process is also likely to be affected by higher rebar temperature. Further investigations to microscopically quantify the heated bar effect should be carried out.

3. PFA is not recommended as a partial substitute for cement to reduce the heated bar effect in the corrosion of carbonated concrete. Both the carbonation and corrosion rates are found to significantly increase when PFA is used to partially substitute cement. Further efforts should be made in future studies to mitigate the heated bar effect on corrosion degradation of carbonated concrete in an economical and sustainable way.

6. Acknowledgement

The financial support from the Seed Fund for Basic Research (2019) by The University of Hong Kong is gratefully acknowledged.

References

[1] U.M. Angst, M.R. Geiker, A. Michel, C. Gehlen, H. Wong, O.B. Isgor, B. Elsener, C.M. Hansson, R. François, K. Hornbostel, R. Polder, M.C. Alonso, M. Sanchez, M.J. Correia, M. Criado, A. Sagüés, N. Buenfeld, The steel–concrete interface, Mater. Struct. 50(2) (2017).https://doi.org/10.1617/s11527-017-1010-1.

[2] A.T. Horne, I.G. Richardson, R.M.D. Brydson, Quantitative analysis of the microstructure of interfaces in steel reinforced concrete, Cem. Concr. Res. 37(12) (2007) 1613-1623.https://doi.org/10.1016/j.cemconres.2007.08.026.
[3] T.A. Soylev, R. François, Quality of steel–concrete interface and corrosion of reinforcing steel, Cem. Concr. Res. 33(9) (2003) 1407-1415.https://doi.org/10.1016/s0008-8846(03)00087-5.
[4] P.R. Jeanty, D. Mitchell, M.S. Mirza, Investigation of top bar effects in beams, ACI Struct. J. 85(3) (1988) 251-257.https://doi.org/10.14359/2613.
[5] R. Zhang, A. Castel, R. François, Influence of steel–concrete interface defects owing to the top-bar effect on the chloride-induced corrosion of reinforcement, Mag. Concr. Res. 63(10) (2011) 773-781.https://doi.org/10.1680/macr.2011.63.10.773.
[6] A. Nasser, A. Clément, S. Laurens, A. Castel, Influence of steel–concrete interface condition on galvanic corrosion currents in carbonated concrete, Corros. Sci. 52(9) (2010) 2878-2890.https://doi.org/10.1016/j.corsci.2010.04.037.
[7] M.G. Sohail, S. Laurens, F. Deby, J.P. Balayssac, Significance of macrocell corrosion of reinforcing steel in partially carbonated concrete: numerical and experimental investigation, Mater. Struct. 48(1-2) (2013) 217-233.https://doi.org/10.1617/s11527-013-0178-2.
[8] T.A. Soylev, R. Francois, Corrosion of reinforcement in relation to presence of defects at the interface between steel and concrete, J. Mater. Civ. Eng. 17(4) (2005) 447-455.https://doi.org/10.1061/(Asce)0899-1561(2005)17:4(447).
[9] A.R. Pati. (2010). Effects of rebar temperature and water to cement ratio on rebar-concrete bond strength of concrete containing fly ash. (Master of Science Thesis). University of North Texas, Retrieved from https://pdfs.semanticscholar.org/ed09/c2d0f5aade36614d9c9926a405fe0d10fbb2.pdf
[10] A. Fahim, P. Ghods, R. Alizadeh, M. Salehi, S. Decarufel, CEPRA: A New Test Method for Rebar Corrosion Rate Measurement, Advances in Electrochemical Techniques for Corrosion Monitoring and Laboratory Corrosion Measurements, ASTM International, 2019. https://www.astm.org/DIGITAL_LIBRARY/STP/PAGES/STP160920170227.htm
[11] M. Stern, A.L. Geary, Electrochemical polarization I. A theoretical analysis of the shape of polarization curves, J. Electrochem. Soc. 104(1) (1957) 56-63.
[12] C. Andrade, C. Alonso, Test methods for on-site corrosion rate measurement of steel reinforcement in concrete by means of the polarization resistance method, Mater. Struct. 37(9) (2004) 623-643.https://doi.org/10.1007/bf02483292.
[13] F. Leng, N. Feng, X. Lu, An experimental study on the properties of resistance to diffusion of chloride ions of fly ash and blast furnace slag concrete, Cem. Concr. Res. 30(6) (2000) 989-992.https://doi.org/10.1016/s0008-8846(00)00250-7.
[14] H. Yazıcı, The effect of silica fume and high-volume Class C fly ash on mechanical properties, chloride penetration and freeze–thaw resistance of self-compacting concrete, Constr. Build. Mater. 22(4) (2008) 456-462.https://doi.org/10.1016/j.conbuildmat.2007.01.002.
[15] B. Elsener, C. Andrade, J. Gulikers, R. Polder, M. Raupach, Half-cell potential measurements—Potential mapping on reinforced concrete structures, Mater. Struct. 36(7) (2003) 461-471.https://doi.org/10.1007/bf02481526.
[16] ASTM C876-91 R99, Standard Test Method for Half-Cell Potentials of Uncoated Reinforcing-Steel in Concrete, ASTM West Conshohocken, PA, 2005.https://doi.org/10.1520/c0876.
[17] R. Polder, C. Andrade, B. Elsener, Ø. Vennesland, J. Gulikers, R. Weidert, M. Raupach, Test methods for on site measurement of resistivity of concrete, Mater. Struct. 33(10) (2000) 603-611.https://doi.org/10.1007/bf02480599.
[18] V.G. Papadakis, Effect of supplementary cementing materials on concrete resistance

against carbonation and chloride ingress, Cem. Concr. Res. 30(2) (2000) 291-299.https://doi.org/10.1016/S0008-8846(99)00249-5.
[19] K.M. Smith, A.J. Schokker, P.J. Tikalsky, Performance of supplementary cementitious materials in concrete resistivity and corrosion monitoring evaluations, ACI Mater. J. 101(5) (2004) 385-390.https://doi.org/10.14359/13424
[20] B. Šavija, M. Luković, Carbonation of cement paste: Understanding, challenges, and opportunities, Constr. Build. Mater. 117 (2016) 285-301.https://doi.org/10.1016/j.conbuildmat.2016.04.138.
[21] P.I.I. Banea. (2015). The study of electrical resistivity of mature concrete. (Master of Science Thesis). Delft University of Technology, Retrieved from https://scholar.google.com/scholar_lookup?title=Study%20of%20Electrical%20Resistivity%20of%20Mature%20Concrete&author=P.I.I.%20Banea&publication_year=2015
[22] S. Lammertijn, N. De Belie, Porosity, gas permeability, carbonation and their interaction in high-volume fly ash concrete, Mag. Concr. Res. 60(7) (2008) 535-545.https://doi.org/10.1680/macr.2008.60.7.535.
[23] M. Stefanoni, U. Angst, B. Elsener, Corrosion rate of carbon steel in carbonated concrete – A critical review, Cem. Concr. Res. 103 (2018) 35-48.https://doi.org/10.1016/j.cemconres.2017.10.007.
[24] G.K. Glass, C.L. Page, N.R. Short, Factors Affecting the Corrosion Rate of Steel in Carbonated Mortars, Corros. Sci. 32(12) (1991) 1283-1294.https://doi.org/10.1016/0010-938x(91)90048-T.
[25] R.W. Revie, Corrosion and corrosion control: an introduction to corrosion science and engineering, John Wiley & Sons2008.
[26] C. Andrade, R. Buják, Effects of some mineral additions to Portland cement on reinforcement corrosion, Cem. Concr. Res. 53 (2013) 59-67.https://doi.org/10.1016/j.cemconres.2013.06.004.
[27] R. Dhir, M. Jones, M. McCarthy, Pulverized-fuel ash concrete: Carbonation-induced reinforcement corrosion rates, Proc. Inst. Civ. Eng. Struct. Build. 94(3) (1992) 335-342.https://doi.org/10.1680/istbu.1992.20293.
[28] T. Hemalatha, A. Ramaswamy, A review on fly ash characteristics – Towards promoting high volume utilization in developing sustainable concrete, J. Clean. Prod. 147 (2017) 546-559.https://doi.org/10.1016/j.jclepro.2017.01.114.
[29] G. Xu, X. Shi, Characteristics and applications of fly ash as a sustainable construction material: A state-of-the-art review, Resour. Conserv. Recy. 136 (2018) 95-109.https://doi.org/10.1016/j.resconrec.2018.04.010.
[30] C.-Q. Lye, R.K. Dhir, G.S. Ghataora, Carbonation resistance of fly ash concrete, Mag. Concr. Res. 67(21) (2015) 1150-1178.https://doi.org/10.1680/macr.15.00204.
[31] P. Sulapha, S.F. Wong, T.H. Wee, S. Swaddiwudhipong, Carbonation of concrete containing mineral admixtures, J. Mater. Civ. Eng. 15(2) (2003) 134-143.https://doi.org/10.1061/(Asce)0899-1561(2003)15:2(134).
[32] R. Felicetti. (2010). Analysis of sorted powder samples for the assessment of deteriorated concrete. Paper presented at the Proc. 6th Int. Conf. on Concrete under Severe Conditions—Environment and Loading (CONSEC'10).https://doi.org/10.1201/b10552-147

Table 1 Characterization of test specimens

Group-specimen Number	PFA replacement level (%)	Water-binder ratio	Depassivated rebar cast temperature (℃)	Passivated rebar cast temperature (℃)
1-1	0	0.60	Ambient	Ambient
1-2	0	0.60	70	
2-1	0	1.0	Ambient	
2-2	0	1.0	50	
3-1	0	0.60	70	
3-2	50	0.60	70	

Table 2 Chemical composition of ordinary Portland cement (OPC) and PFA

Binder	CaO	SiO_2	Al_2O_3	Fe_2O_3	MgO	SO_3	Na_2O
52.5N OPC	67.0%	21.2%	5.8%	3.3%	0.7%	2.8%	0.46%
PFA	1.5%	58.0%	30.0%	4.3%	2.8%	-	3.2%

Table 3 Mix proportion of concrete

Group-specimen Number	Water (kg/m^3)	Cement (kg/m^3)	PFA (kg/m^3)	Crushed gravel (kg/m^3)	Sand (kg/m^3)	Maximum gravel size (mm)
1-1、1-2	230	383	0	614.9	1142.1	10
2-1、2-2	350	350	0	868	972	20
3-1	210	350	0	868	972	20
3-2	210	175	175	868	972	20

Table 4 Interpretation of corrosion rate to corrosion level according to RILEM [12]

Corrosion level	Negligible	Low	Moderate	High
Corrosion rate (uA/cm^2)	<0.1	0.1-0.5	0.5-1.0	>1.0

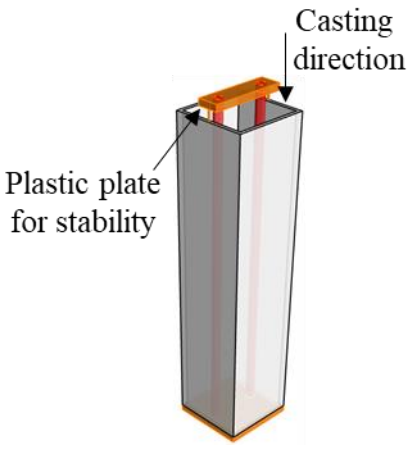

(a)

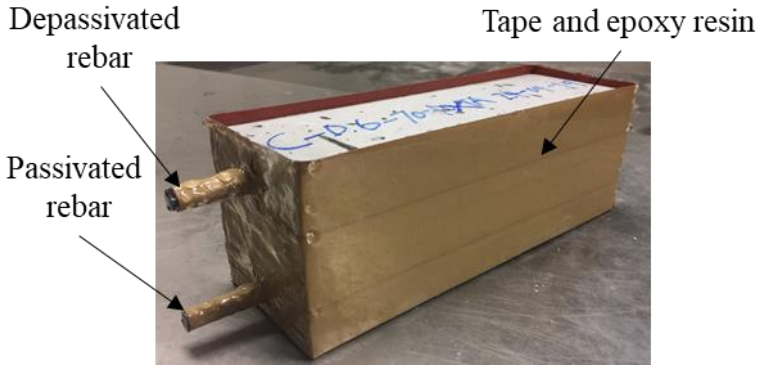

(b)

Figure 1 Specimen preparation: (a) Vertical casting to prevent top bar effect (b) Tape and epoxy resin coating to ensure CO_2 penetration into bottom surface

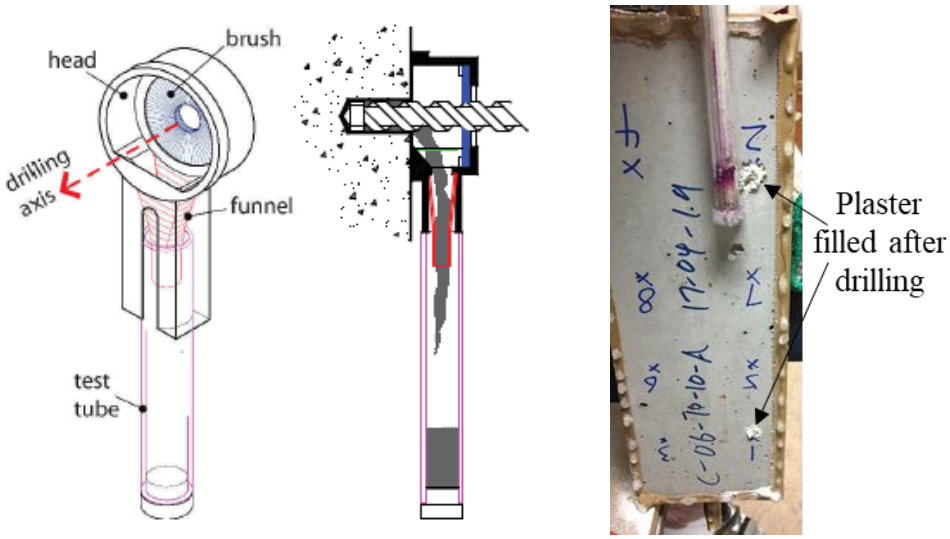

(a) Funnel and test tube[32] (b) Drilling[32] (c)Plaster refillment

Figure 2 Carbonation depth test on additional specimen

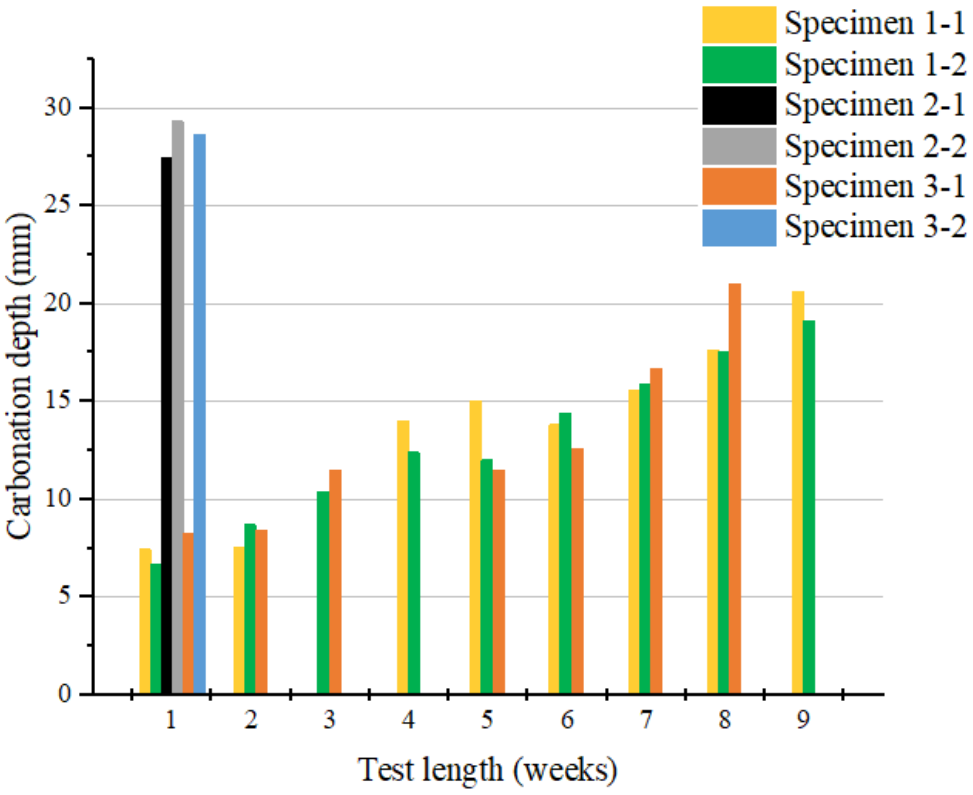

Figure 3 Changes in carbonation depth over time

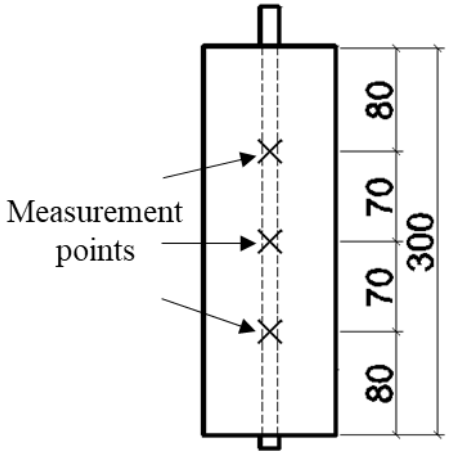

Figure 4 Longitudinal points of measurement on specimen

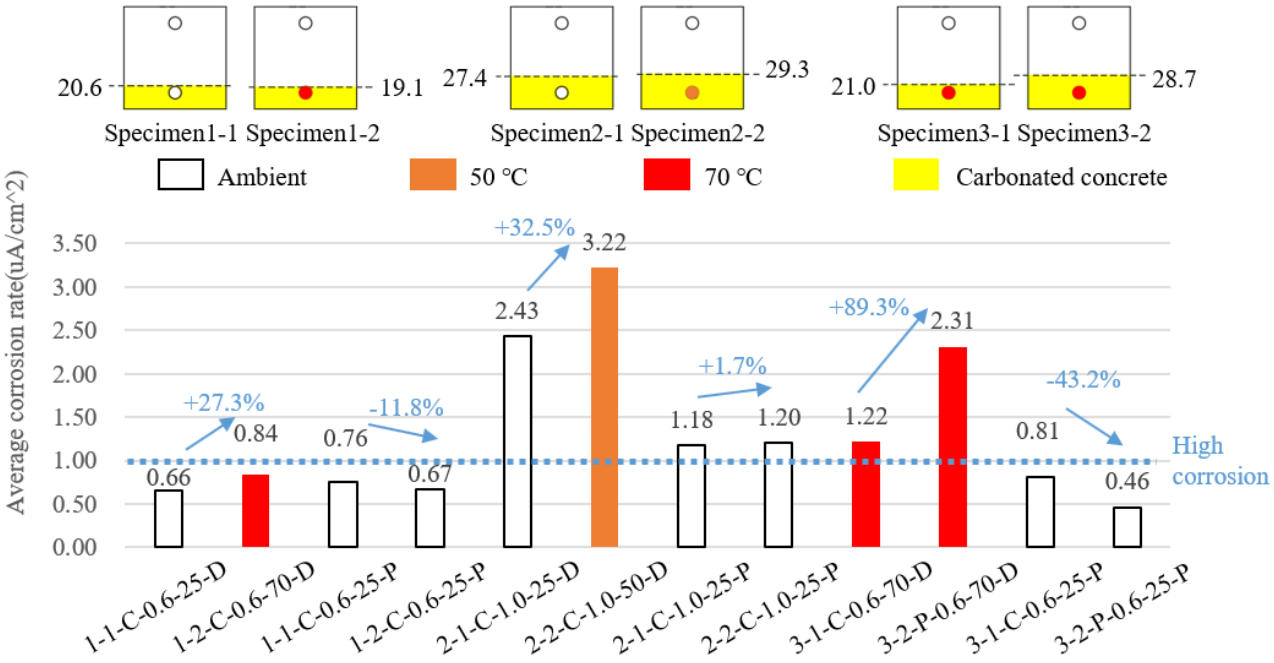

Figure 5 Comparison of average corrosion rate of rebars (Unit for carbonation depth: mm) Note: The rebars are labelled according to "Specimen number"-"Cement type"-"W/B ratio"-"Rebar temperature"-"Depassivation state". C means OPC; P means OPC partially replaced by PFA; 25 means ambient temperature; D means depassivated rebar; P means passivated rebar.

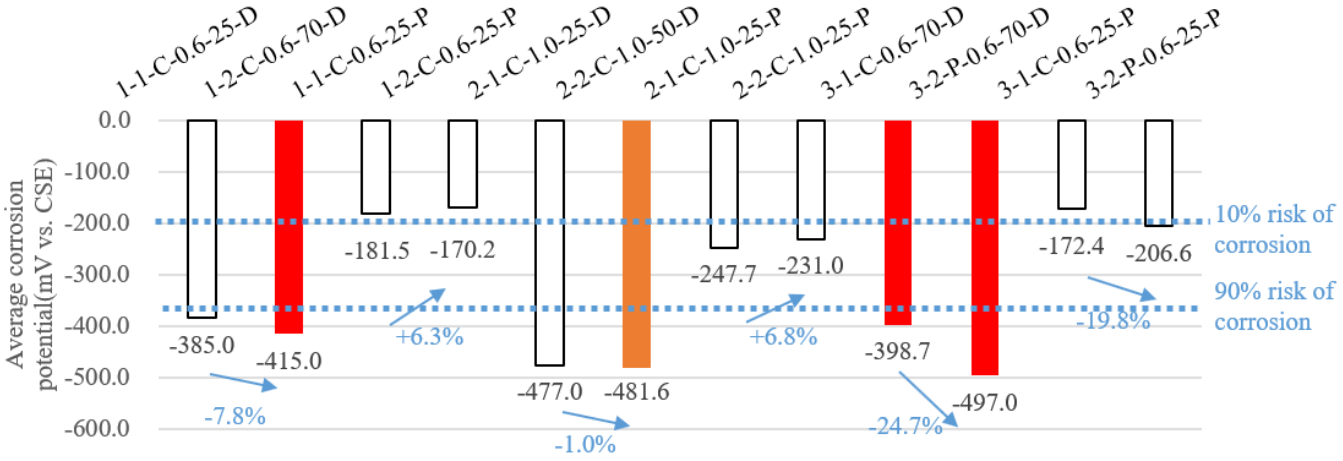

Figure 6 Comparison of average corrosion potential of rebars

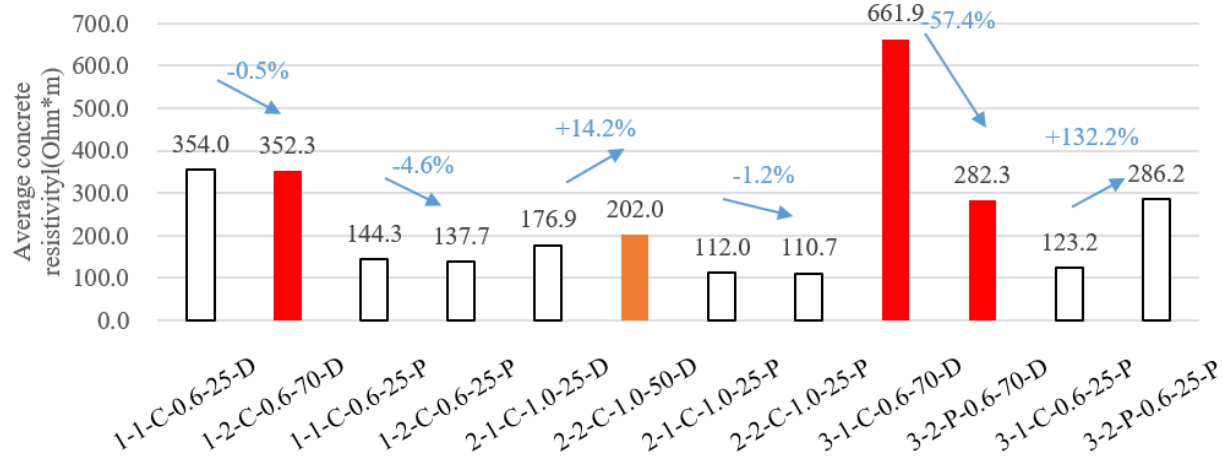

Figure 7 Comparison of average concrete resistivity at top and bottom surfaces

* *Corresponding author, Email: klsu@hku.hk, Tel no.: +852 2859 2648*

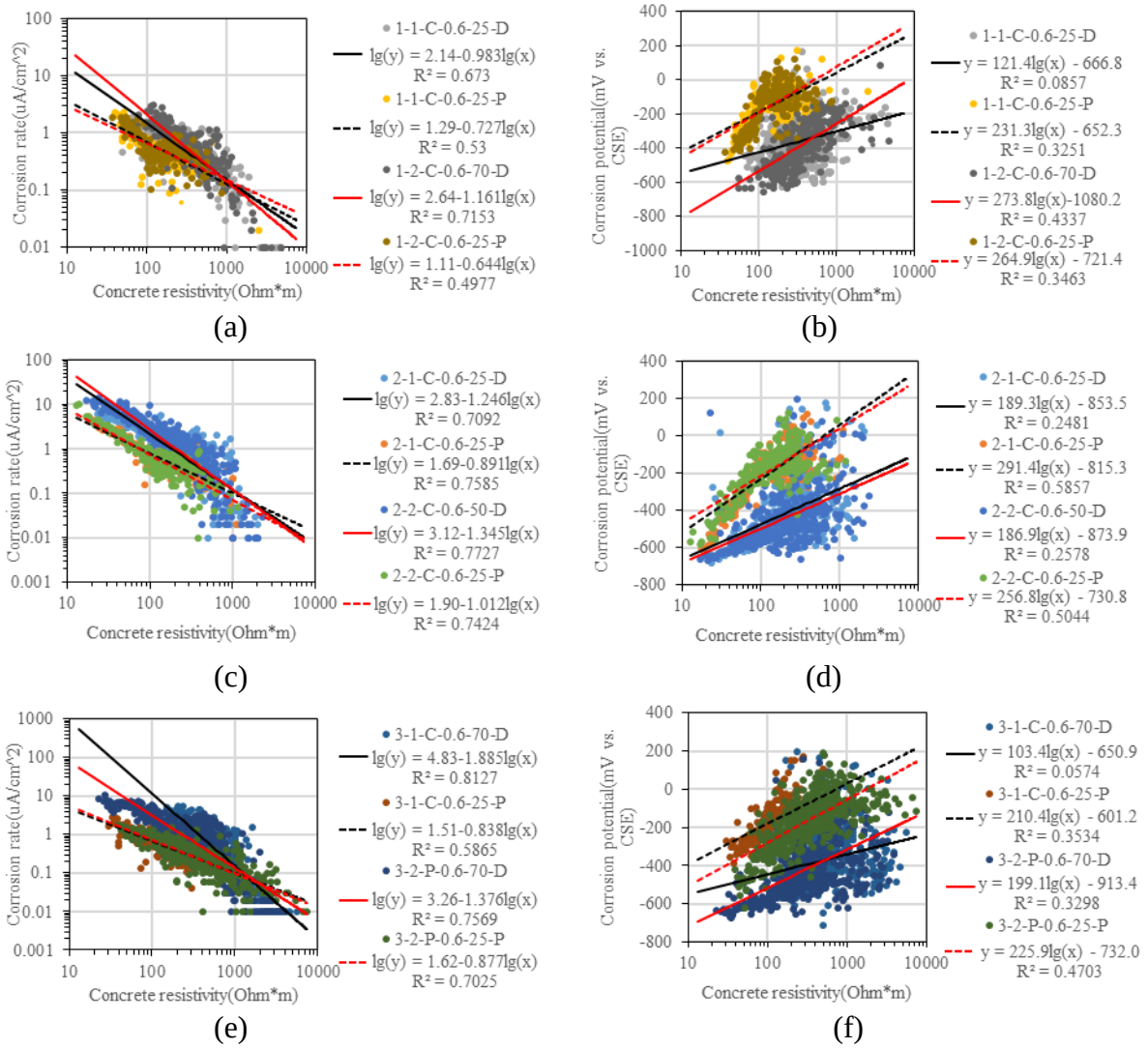

Figure 8 Correlations among corrosion rate, corrosion potential and concrete resistivity: (a) and (b) Group 1; (c) and (d) Group 2; and (e) and (f) Group 3. Solid/dashed regression lines indicate depassivated/passivated rebars, and regression lines in red/black indicate experimental/reference specimens, respectively

** Corresponding author, Email: klsu@hku.hk, Tel no.: +852 2859 2648*

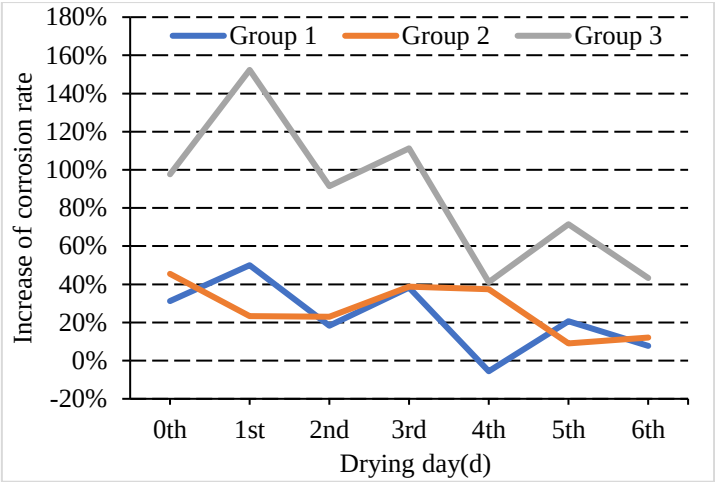

Figure 9 Average increase in corrosion rate on different days of drying period. For each group, increase in corrosion rate means increase in corrosion rate of depassivated rebars (percentage)